

## Fast Simultaneous Thickness Measurements of Gold and Nickel Layers on Copper Substrates

By J. R. MALDONADO and D. MAYDAN

(Manuscript received April 20, 1979)

*The thickness of nickel and gold films plated on a copper substrate has been determined by measuring the intensity of various fluorescent lines excited in reflection by a 50-kV tungsten X-ray source. An exploratory system has been constructed which can simultaneously measure the thickness of the gold and nickel layers on an area of  $125 \times 175 \mu\text{m}$ . Thickness of gold from  $0.2 \mu\text{m}$  to  $5 \mu\text{m}$  and from  $0.3 \mu\text{m}$  to  $1.5 \mu\text{m}$  of nickel can be measured to an accuracy of  $\pm 6$  percent in the gold films and  $\pm 10$  percent in the nickel films in about 20 seconds, including the measurement and calculation. The equations describing the attenuation of the incident radiation, the primary and secondary excitation of fluorescence radiation in the films, and the attenuation of the fluorescence radiation in the films have been determined for the case of nickel and gold films on copper substrates and for indium and gold films on copper substrates and are solved by a computer in the system. The method could be extended to other multilayer systems.*

### I. INTRODUCTION

With the recent increase in the price of gold and other precious metals, new ways are being investigated to reduce the consumption of these materials. For example, replacing the uniform plating process with the selective electroplating of gold to tailor-fit the gold layer to the small mating surfaces of the contacts in connectors and integrated circuit packaging hardware will result in large savings of gold. With this new approach, monitoring the thickness of the gold and the nickel layer underneath it at relatively high degrees of accuracy and at high speed becomes an important factor in controlling the deposition process.

Today, the most common way to measure the thickness of the gold layer is to use a radioactive beta source which generates high-energy

electrons and then to monitor the backscattered electrons from the gold layer to determine its thickness. Since bright radioactive sources are not available, the system is only adequate for the thickness measurement of materials over 0.5 mm in diameter and with measurement times of 1 min or longer. In addition, the measurement is very sensitive to any change in position of the substrate material relative to the electron detector.

X-ray fluorescence has been used by many authors to determine thickness of both the nickel and gold layers.<sup>1,2</sup> This is done by monitoring the magnitude of the direct fluorescence from the two layers which are excited by a shorter X-ray wavelength. However, as shown in this paper, the fluorescence intensity produced by the gold saturates at gold thicknesses above 3  $\mu\text{m}$ , which limits the useful range of thickness measurements to less than 3  $\mu\text{m}$ . Also, the systems reported in the literature are not capable of simultaneous measurements of nickel and gold films.

We describe in this paper an X-ray fluorescence system for the simultaneous measurement of small areas of gold and nickel layers plated on copper substrates. The system, schematically shown in Fig. 1, consists of an X-ray source with a tungsten or rhenium target operating at 50 kV (less than 1 mA), a 160-eV lithium-doped silicon detector with a specially designed detector collimator and a programmable X-ray analyzer. This system allows us to display the value of the thickness of small areas ( $\sim 100$   $\mu\text{m}$  diameter) of gold and nickel films on copper substrates in times of the order of 20 s and with an accuracy of better than 10 percent.

For the thickness measurement of a thin nickel layer deposited on a copper substrate and a thicker gold layer deposited on top of the nickel, we excite  $\text{K}\alpha_{12}$  lines in the copper and nickel with the broad wavelength spectrum from the X-ray source as shown in Fig. 1. The nickel thickness is determined by the magnitude of the direct fluorescence, while the gold thickness is measured by the attenuation of the  $\text{CuK}\alpha_{12}$  lines passing through the gold film. The  $\text{CuK}\alpha_{12}$  lines are denoted by  $\text{CuK}\alpha$  in this paper.

Experimental results obtained with the X-ray fluorescence system are presented and compared with results obtained by cross-sectioning the samples and determining the thickness by optical means. An extension to other multilayer systems is also presented.

## II. DESCRIPTION OF SYSTEM

### 2.1 Geometry of the system

The X-ray system is shown in Fig. 1. It consists of an X-ray source illuminating the sample, an X-ray detector to detect the fluorescence radiation from the sample with a specially designed detector collimator, and associated electronics. Optical alignment of the samples is also

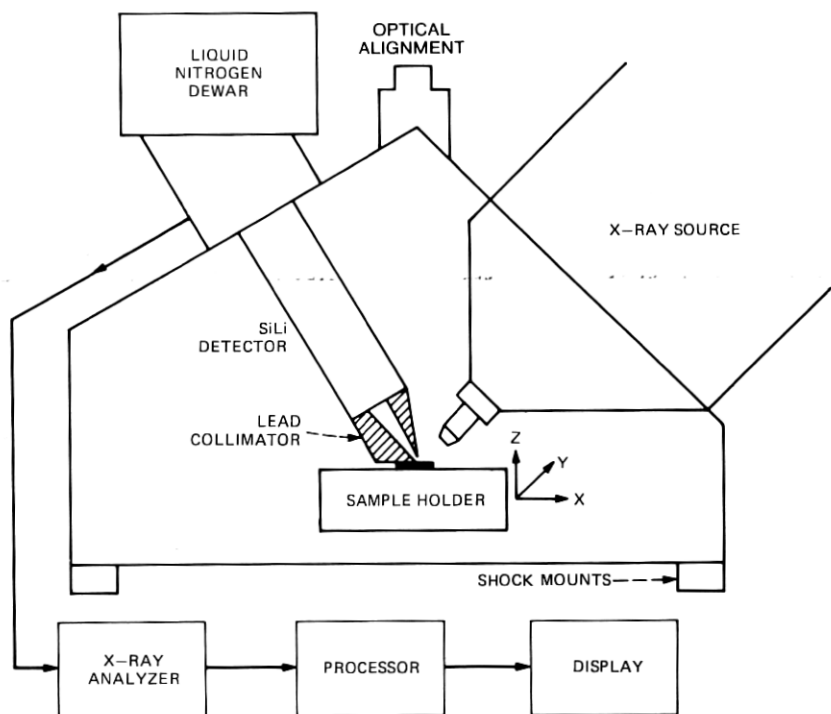


Fig. 1—X-ray system.

provided. The X-ray source incident angle (45 degrees) was chosen to minimize the interaction of the different layers due to the attenuation of the incident beam and also to allow for optical registration. The detector angle (30 degrees) (fluorescent angle measured from the normal to the surface) was chosen to minimize the attenuation of the  $\text{NiK}\alpha$  line in the gold film and also to allow for the thickness measurement of relatively thick gold films (4 to 5  $\mu\text{m}$ ). If optical alignment can be obtained from the backside of the sample, the reflection angle could be reduced to 0. This will increase the thickness measuring range of the gold films and increase the counting accuracy of the nickel films.

In operation (shown in Fig. 2), the X-ray output from the tube is collimated by a dual lead collimator (shown in Fig. 2), about 2 mm in diameter (each path) and 1 cm long. The beam collimated normal to the beryllium window is used for X-ray fluorescence excitation of the sample (i.e.,  $\text{CuK}\alpha$ ,  $\text{NiK}\alpha$ , and  $\text{AuL}\alpha$ ). The second beam induces fluorescence in the lead collimator on the detector. To determine the thicknesses of the gold and nickel layers, the magnitude of the  $\text{CuK}\alpha$  and  $\text{NiK}\alpha$  lines from the sample are compared with the corresponding lines obtained from thick copper and nickel samples. The  $\text{PbL}\beta$  line is used as a reference signal to account for variations in the X-ray flux

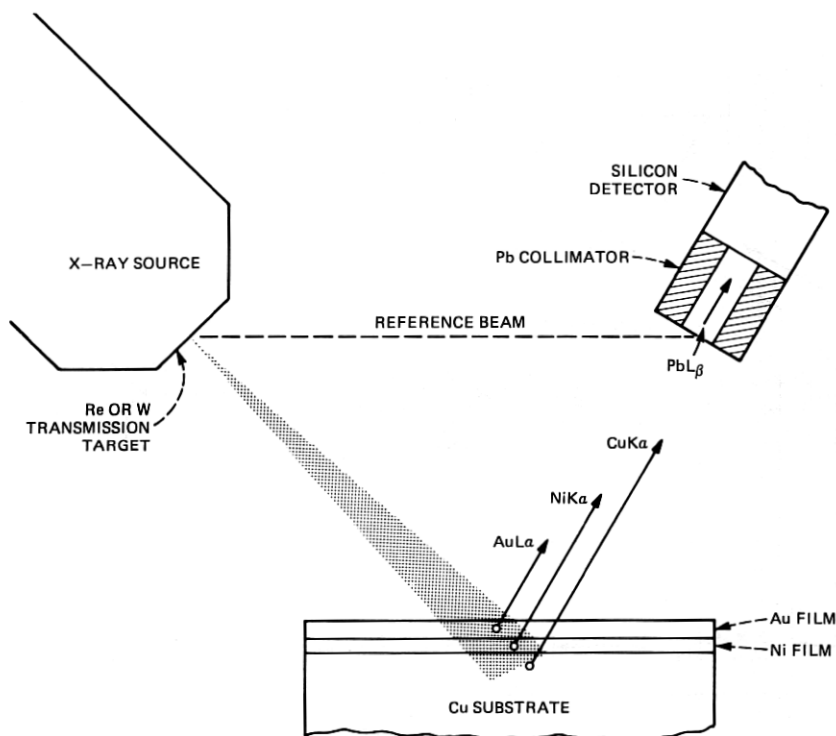


Fig. 2—Thickness measurement technique. The magnitude of the fluorescent lines from the sample ( $\text{CuK}\alpha$ ),  $\text{NiK}\alpha$ , and  $\text{AuL}\alpha$ , excited by the X-ray source, are measured by the silicon detector and the X-ray analyzer. The magnitude of those fluorescent lines is compared with the magnitude of the fluorescent lines obtained with thick layers of copper and nickel. The thickness of the gold and nickel layers is obtained by solving a system of two nonlinear equations with two unknowns in the computer built in the X-ray analyzer. The  $\text{PbL}\beta$  line from the detector X-ray collimator is used to compensate for source intensity variations.

from the source. The presence of the  $\text{PbL}\beta$  line increases the input count rate to the system. Therefore, some trade-off is needed in the magnitude of the  $\text{PbL}\beta$  line and the minimum measurement time. In our present setup, the  $\text{PbL}\beta$  line is not needed if the system is calibrated once a day. X-ray flux variations from one day to another are typically less than 2 percent for the counting statistics of our experiments.

## 2.2 X-ray source

The system X-ray source is manufactured by Watkins Johnson, with a tungsten or rhenium target capable of operating at 1 mA maximum current from 10 kV to 75 kV. The power supply regulation is better than 1 percent, and the long-term stability of the system is  $\pm 3\sigma$ , ( $\sigma \approx (1/\sqrt{N})$ ), where  $\sigma$  is the standard deviation and  $N$  is the number of



counts in the detector. The electron beam spot size is less than 2 mm in diameter.

We have considered two kinds of X-ray sources, a reflection tube and a transmission tube. The experimental results reported here were performed with a conventional 50-kV solid tungsten target reflection tube with a side-mounted Be window. The transmission tube (schematically shown in Fig. 1), manufactured by Watkins Johnson to our specifications, consists of a 10- $\mu$ m thick rhenium or tungsten dot about 3 mm in diameter deposited on a 250- $\mu$ m thick beryllium foil about 1.25 cm in diameter. This geometry allows the target to be located very close to the sample (<2 cm) to maximize the X-ray flux and reduce the measuring time. However, the fluorescence excitation obtained from the transmission tube was considerably lower than the one produced by the side window tube.

### **2.3 X-ray detector and electronics**

The X-ray detector is a conventional nitrogen-cooled, lithium-doped silicon detector (3 mm thick), manufactured by PGT (Princeton Gamma Tech). The effective detector diameter is 4 mm and the detector-to-window distance is 3 mm. In order to reduce the detector-to-sample distance, the detector nozzle diameter is about 16 mm.

After being amplified and processed by proper pileup rejection, the detector output is fed into a PGT 1000 multichannel analyzer. The analyzer has 16 kbits of memory and two floppy disks (256,000 words). The disks are used for basic programs and thickness calculations. The analyzer allows for qualitative analysis with automatic element identification. The system has the capability of performing quantitative analysis with appropriate software. If analysis of elements with  $Z < 13$  is required, the system may be operated in vacuum or in a helium chamber.

### **2.4 Detector collimator**

A typical lead collimator used on the 16-mm diameter detector nozzle is shown in Fig. 3. It consists of a truncated conical hole (in the lead piece) of about 1.7 cm long. The collimator is constructed by casting lead in an appropriate mold. This shape was chosen to maximize the detector solid angle. The smallest aperture in the cone is about 100  $\mu$ m in diameter, and the largest aperture is about 3.5 mm in diameter. In operation, the sample is placed in contact with one of the surfaces of the lead piece. This surface is covered with a smooth surface (like glass), as shown in Fig. 3. The excited fluorescence from the sample is transmitted to the detector through the collimator. Therefore, the collimator serves two purposes: (i) it maximizes the fluorescence signal reaching the detector from a small area on the

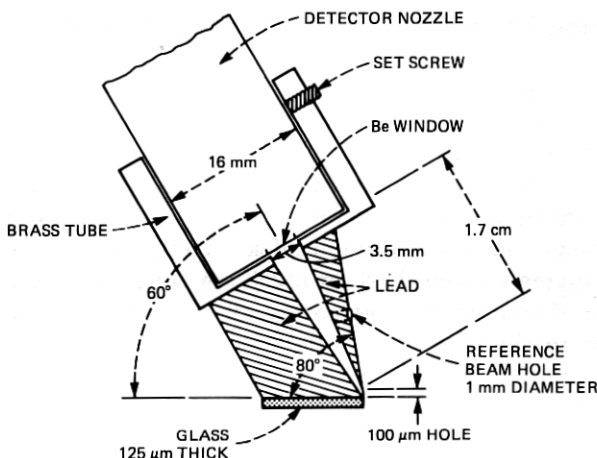


Fig. 3—Detector collimator.

sample and (ii) it determines the distance from sample to detector to minimize geometrical errors. The average distance from the 100- $\mu$ m aperture in the collimator to the sample is about 100  $\mu$ m.

### 2.5 Optical alignment

In our prototype system, the alignment is performed under a microscope by removing the collimator from the detector. The alignment also may be performed optically by means of a telescope (shown in Fig. 1) and an XYZ positioner. In this arrangement, the sample may be moved in the XY plane against the glass surface of the collimator by means of the XYZ positioner. The collimator is provided with a fiducial mark (arrow) next to the 100- $\mu$ m aperture to optically align the sample relative to the mark.

## III. SYSTEM CONSIDERATIONS

To study the feasibility of the X-ray fluorescence system for the fast thickness measurement of small areas of gold and nickel on copper substrates, we needed an estimate of the required X-ray flux from the source. For this purpose, we calculated the magnitude of the  $\text{CuK}\alpha$  lines from the substrate attenuated by the gold film. The calculations are presented in Appendix A using the model shown in Fig. 4. The results are shown in Fig. 5 normalized to the tube current and solid angles  $\sigma_{\text{in}}$ ,  $\sigma_{\text{out}}$  defined in Fig. 4. The calculations for the  $\text{AuL}\alpha$  radiation are presented in Appendix B, and the results are also shown in Fig. 5. For the case of a 1-mm diameter source, placed 10 mm away from a 100- $\mu$ m diameter sample, with a sample-to-detector (12  $\text{mm}^2$ ) distance of 20 mm, we get  $\sigma_{\text{in}}\sigma_{\text{out}} \approx 1.2 \times 10^{-6}$ . For a 3.4  $\mu$ m gold film (using the

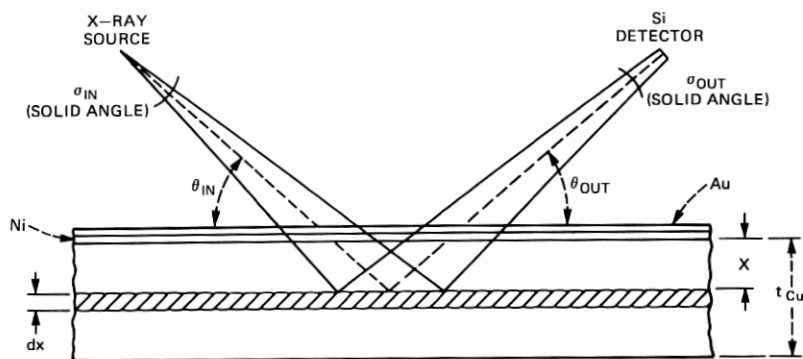


Fig. 4—Model used for calculations in the X-ray fluorescence system.

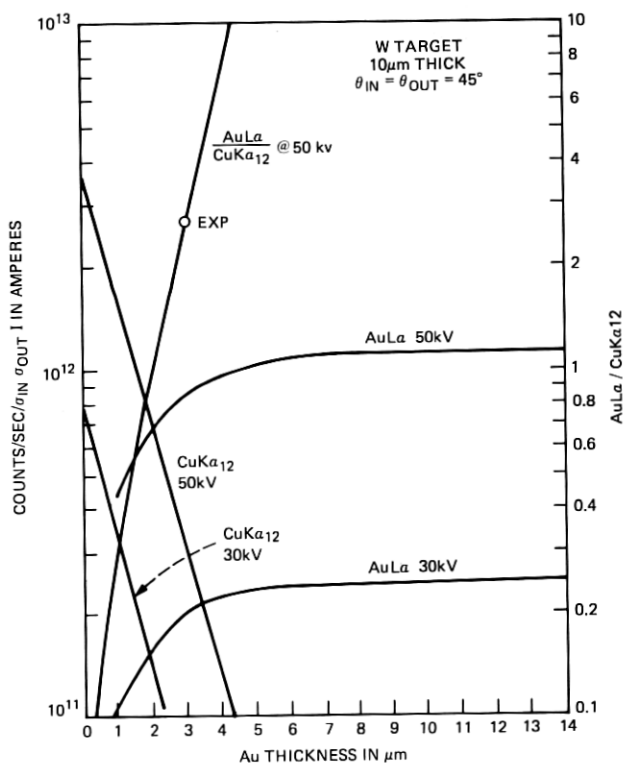


Fig. 5—Calculated counting rate/ $\sigma_{in}\sigma_{out} I$  (amps) of the  $CuK\alpha_{12}$  lines vs gold thickness at two different target voltages. The calculated counting rate/ $\sigma_{in}\sigma_{out} I$  (amp) of the AuLa line vs gold thickness is also shown. The ratio of AuLa/ $CuK\alpha_{12}$  lines is also shown in the figure. This ratio is independent of the input and output solid angles and the tube current. An experimental point is included in the figure to show the excellent agreement with the calculated value.

geometry described above), we get from Fig. 5 that a 1-mA, 50-kV tungsten tube, with a 10- $\mu$ m tungsten filter, will produce about 360 counts/s of  $\text{CuK}\alpha$  radiation at the detector. In practice (with no tungsten filter), because of the simultaneous presence of the  $\text{NiK}$  lines, the  $\text{AuL}$  lines, and the background radiation, the total count rate reaching the detector is considerably higher (a factor of 10 or more). Therefore, for a 1-mA tube current, the analyzer will have to handle count rates larger than 3500 counts/s. The programmable analyzer used in our system could process only about 3500 counts/s (6- $\mu$ s time constant) with a 50-percent dead time; hence, the minimum counting time is limited by the analyzer and not by the X-ray source. To get good statistics (less than 5 percent error) in the  $\text{NiK}\alpha$  line when measuring thin nickel films (less than 1  $\mu$ m) under thick gold films (about 3  $\mu$ m), it is necessary to have a counting time of about 20 s (real time, about 10 s lifetime). This performance is achieved using about 0.5 mA tube current with no tungsten filter. Shorter measuring times are possible if larger standard deviations are tolerable or when only gold films are present. In the last case, for gold films larger than 2  $\mu$ m, only 1 or 3 s (real time) are needed. For thinner gold films, the statistical error in the  $\text{CuK}\alpha$  is relatively small; however, the change in gold thickness for a given change in the counting rate is larger than for the case of thick gold films, as can be observed from Fig. 5. Therefore, for measuring thin gold films, a somewhat longer counting time is necessary if accuracies of less than 3 percent are desired. In our present system, a 5-s counting time is used for measuring single gold films larger than 0.4  $\mu$ m for counting accuracies of about 5 percent.

#### IV. SIMULTANEOUS THICKNESS DETERMINATION OF TWO-LAYER SYSTEMS

##### 4.1 Gold and nickel films

To minimize the interaction between the metallic layers, we have considered using a suitable filter in the source to provide a spectrum peaking at high energies (above 30 kV). However, doing this requires the penalty of having a lower fluorescence signal generated in the thin layers (in particular, the nickel layers less than 1  $\mu$ m thick) when compared to the case of an unfiltered incident spectrum. The presence of the WL lines and the low energy background radiation from the X-ray source increases the  $\text{NiK}\alpha$  fluorescence due to the high absorption of nickel at those energies. Therefore, in order to increase the accuracy of our measurements, we are presently using a reflection system with an unfiltered tungsten target capable of efficient generation of X-ray energy down to a few kilovolts. Under these conditions, the interaction between the layers can occur in two ways: (i) by one layer (or layers) absorbing incident radiation effective for excitation of fluorescence in

another layer underneath; or (ii) by secondary fluorescence (this case is always present independent of the incident spectrum) that occurs when fluorescence lines excited in one layer induce fluorescence in other layers (increasing the total fluorescent radiation from this layer).

In the case of the gold-nickel-copper system, the thickness of the top gold layer affects the fluorescence of the nickel and copper layers underneath it in the two ways mentioned above and described in detail below. The incident radiation from the X-ray tube induces  $L$  electron transitions in the gold film. The  $AuL$  lines produced in this manner are absorbed by the nickel film and the copper substrate and induce  $NiK\alpha$  and  $CuK\alpha$  radiation on both metal layers respectively. This secondary induced radiation adds to the excited radiation induced by the incident beam (attenuated by the gold layer) in the nickel and copper layers and, if not corrected for, gives an apparent increase in the nickel thickness. Furthermore, as mentioned before, the  $WL\alpha$  line, from the source (very effective in exciting  $NiK\alpha$  radiation) is reduced in amplitude by the gold layer. Therefore, as the gold thickness increases, we expect a large decrease in attenuation of the incident radiation effective to excite the  $NiK\alpha$  line. This is because the spectrum has been filtered and the radiation available for excitation of the  $NiK\alpha$  line now lies at higher energies and is less effective than in the case without gold where the  $WL\alpha$  ( $\sim 8.2$  kV) was the predominant excitation mechanism. As mentioned above, there is also a secondary excitation effect for the  $CuK\alpha$  line due to the gold film fluorescence and also an effect due to the gold film absorption of the incident radiation. However, the energy of the  $WL\alpha$  line is below the copper  $K$  absorption edge and only the continuum radiation (higher energy) contributes to the  $CuK\alpha$  excitation. The effect on the  $CuK\alpha$  line due to the presence of the gold film was found experimentally to be small in the range of Au thickness of interest (0 to 5  $\mu\text{m}$ ).

The calculation of the above interactions is very involved and will not be presented in this paper. Fortunately, the above effects tend to compensate for each other in the range of gold thicknesses below 4  $\mu\text{m}$ , and can be corrected in first order by assuming that the effective absorption coefficient of gold to the  $NiK\alpha$  line decreases linearly with the thickness of the gold layer. For thicker gold films, an exponential correction has been found adequate. For a given geometry of the system, we can write for the attenuation coefficient of gold to the  $NiK\alpha$  line

$$\alpha_{NiK\alpha}^{Au} = \alpha_1 + \alpha_2 t_{Au}, \quad (1)$$

where  $\alpha_1$  and  $\alpha_2$  are determined experimentally. The magnitude of the  $NiK\alpha$  line measured after a gold thickness  $t_{Au}$  is given by the empirical formula

$$\text{NiK}\alpha = \text{NiK}\alpha_{\infty}[1 - \exp(-\alpha_3 t_{\text{Ni}})]\exp(-\alpha_{\text{NiK}\alpha}^{\text{Au}} t_{\text{Au}}), \quad (2)$$

where  $\text{NiK}\alpha_{\infty}$  is the magnitude of the  $\text{NiK}\alpha$  line for a thick Ni plate ( $>25 \mu\text{m}$ ) and an  $\alpha_3$  and an  $\alpha_{\text{NiK}\alpha}^{\text{Au}}$  are experimentally determined parameters.

The magnitude of the  $\text{CuK}\alpha$  line (in a given system) attenuated by the nickel and gold layers is given by

$$\text{CuK}\alpha = \text{CuK}\alpha_{\infty}\exp(-\alpha_{\text{CuK}\alpha}^{\text{Ni}} t_{\text{Ni}})\exp(-\alpha_{\text{CuK}\alpha}^{\text{Au}} t_{\text{Au}}), \quad (3)$$

where  $\text{CuK}\alpha_{\infty}$  is the magnitude of the  $\text{CuK}\alpha$  line obtained from a thick copper plate, and  $\alpha_{\text{CuK}\alpha}^{\text{Ni}}$  and  $\alpha_{\text{CuK}\alpha}^{\text{Au}}$  are the attenuation coefficients of nickel and gold to the  $\text{CuK}\alpha$  line, respectively. It must be clarified at this point that  $\alpha_{\text{CuK}\alpha}^{\text{Au}}$ ,  $\alpha_{\text{NiK}\alpha}^{\text{Au}}$ , and  $\alpha_{\text{CuK}\alpha}^{\text{Ni}}$  include the attenuation of the incident X-ray beam as well as the attenuation by the gold or nickel layer of the excited fluorescent beam, and depend on the geometry of the system.

Because the  $\text{NiK}\beta$  line is very close in energy to the  $\text{CuK}\alpha$  line it is necessary to correct the measured  $\text{CuK}\alpha$  line  $\text{CuK}\alpha_M$  in the following way:

$$\text{CuK}\alpha = \text{CuK}\alpha_M - \alpha_5 \text{NiK}\alpha[1 + (\alpha_{\text{NiK}\alpha}^{\text{Au}} - \alpha_{\text{CuK}\alpha}^{\text{Au}})t_{\text{Au}}], \quad (4)$$

where  $\alpha_5$  is determined experimentally by measuring the number of counts in the  $\text{CuK}\alpha$  window produced by a pure nickel sample, and knowing the ratio  $\text{NiK}\beta/\text{NiK}\alpha$ . The quantity in parenthesis corrects by the difference in absorption for the  $\text{CuK}\alpha$  and  $\text{NiK}\alpha$  lines in gold. Typically,  $\alpha_5 \approx 0.037$  and  $\alpha_{\text{NiK}\alpha}^{\text{Au}} - \alpha_{\text{CuK}\alpha}^{\text{Au}} \approx 0.08$  (average).

From eqs. (1) to (4) we can solve for the nickel and gold thicknesses:

$$t_{\text{Ni}} = \frac{1}{\alpha_3} \ln \left( 1 - \frac{\text{NiK}\alpha}{\text{NiK}\alpha_{\infty}} \exp \alpha_{\text{NiK}\alpha}^{\text{Au}} t_{\text{Au}} \right)^{-1} \quad (5)$$

$$t_{\text{Au}} = \frac{1}{\alpha_{\text{CuK}\alpha}^{\text{Au}}} \ln \left( \frac{\text{CuK}\alpha_{\infty} \exp(-\alpha_{\text{CuK}\alpha}^{\text{Ni}} t_{\text{Ni}})}{\text{CuK}\alpha_M - \alpha_5 \text{NiK}\alpha[1 + (\alpha_{\text{NiK}\alpha}^{\text{Au}} - \alpha_{\text{CuK}\alpha}^{\text{Au}})t_{\text{Au}}]} \right). \quad (6)$$

Equations (5) and (6) may be solved by successive iterations taking the initial value of  $t_{\text{Au}} = t_{\text{AUF}}$ , where  $t_{\text{AUF}}$  is the thickness of gold film\* obtained by direct fluorescence:

$$t_{\text{AUF}} = \frac{1}{\alpha_6} \ln \left[ 1 - \frac{\text{AuL}\alpha}{\text{AuL}\alpha_{\infty}} \right]^{-1}, \quad (7)$$

\* Although the iteration could be started from any initial value of  $t_{\text{AUF}}$ , the value of  $t_{\text{AUF}}$  obtained from eq. (7) is very useful when measuring gold thin films less than  $1 \mu\text{m}$  thick. If the value of  $t_{\text{Au}}$  [obtained by eq. (6)]  $\ll t_{\text{AUF}}$ , the thin film is suspected of having a large pinhole density.

where  $AuL\alpha_{\infty}$  is the magnitude of the  $AuL\alpha$  line for a thick gold film ( $>10 \mu m$ ) and  $\alpha_6$  is determined experimentally. In addition, by manipulating eqs. (2), (3), and (7) it is possible to obtain a system of two equations with two unknowns that involve the ratio of the fluorescent lines to the  $CuK\alpha$  line. These equations are independent of the geometrical and intensity variations of the measuring apparatus.

These equations are:

$$t_{Ni} = \frac{1}{\alpha_{CuK\alpha}^{Ni}} \ln \frac{AuL\alpha_{\infty}}{CuK\alpha} \frac{CuK\alpha_{\infty}}{AuL\alpha_{\infty}} [1 - \exp(-\alpha_6 t_{Au})]^{-1} \times \exp(-\alpha_{CuK\alpha}^{Au} t_{Au}) \quad (5')$$

$$t_{Au} = \frac{1}{\alpha_{CuK\alpha}^{Au} - \alpha_{NiK\alpha}^{Au}} \ln \frac{NiK\alpha}{CuK\alpha} \frac{CuK\alpha_{\infty}}{NiK\alpha_{\infty}} \frac{\exp(-\alpha_{CuK\alpha}^{Ni} t_{Ni})}{1 - \exp(-\alpha_3 t_{Ni})}, \quad (6')$$

where  $\alpha_{NiK\alpha}^{Au}$  is given by (1) and  $CuK\alpha$  is given by eq. (4). However, the experimental results presented in this paper were not obtained using eqs. (5') and (6'). A value for  $t_{AuF}$  can also be found by the ratio of the  $AuL\alpha/CuK\alpha$  when the nickel thickness is small as shown in Fig. 3, and also by the ratio of  $AuL\alpha/AuM\alpha_{12}$  for any thickness of nickel (providing a calibration curve for  $AuL\alpha/AuM\alpha_{12}$  vs  $t_{Au}$  is obtained). The determination of the Au thickness by the ratio of  $AuL\alpha/AuM\alpha_{12}$  could prove to be an effective technique, assuming that enough counts are obtained in the  $AuM\alpha_{12}$  line for a desired measurement time. The  $AuM\alpha_{12}$  is attenuated somewhat by the air between the detector and the sample. (This attenuation can be taken care of in the calibration of  $t_{Au}$  vs  $AuL\alpha/AuM\alpha_{12}$ ). This correction may not be necessary if the full fluorescence analysis capability (detection of elements with  $<13$ ) of the system are utilized by filling the sample chamber with helium or operating under vacuum. The use for the  $AuL\alpha/AuM\alpha_{12}$  ratio in determining the gold thickness is essential for determining the thickness of gold-nickel and copper layers on some other substrate, as discussed below.

## 4.2 Measurements of other metallic layers

### 4.2.1 The three-layer system: gold-nickel-copper

Using the fluorescence technique, it is possible to determine the thickness of gold on nickel on copper layers ( $<10 \mu m$ ) on unknown thickness palladium substrates. The gold thickness ( $t_{Au}$ ) is first determined by the  $AuL\alpha/AuM\alpha_{12}$  ratio from a previously determined dependence. The thickness of the nickel and copper layers is then determined by the direct fluorescence of those layers attenuated by the layers above.

The fluorescence  $K\alpha$  radiation in a given system due to the copper layer is given by

$$\text{CuK}\alpha = \text{CuK}\alpha_{\infty}[1 - \exp(-\beta t_{\text{Cu}})]\exp(-\alpha_{\text{CuK}\alpha}^{\text{Ni}} t_{\text{Ni}})\exp(-\alpha_{\text{CuK}\alpha}^{\text{Au}} t_{\text{Au}}), \quad (8)$$

where  $\beta$  is a parameter determined experimentally.

The magnitude of the  $\text{NiK}\alpha$  line is given by eq. (2). Using eq. (4) to correct for the measured ( $\text{CuK}\alpha_{\text{M}}$ ) and eq. (1) for other corrections, we get a system of two equations, (2) and (8) with two unknowns,  $t_{\text{Ni}}$  and  $t_{\text{Cu}}$ . Equation (2) can be directly solved for  $t_{\text{Ni}}$ , knowing  $t_{\text{Au}}$  (from above) and eq. (8) can then be solved for  $t_{\text{Cu}}$ .

In all the above calculations we have neglected the effect of the  $\text{CuK}\beta$  line on producing  $\text{NiK}\alpha$  fluorescence. This effect is lumped in  $\alpha_{\text{NiK}\alpha}^{\text{Au}}$  given in eq. (1).

#### 4.2.2 The two-layer system: gold and indium on thick copper substrates

The thicknesses of the gold and indium layers can be obtained in two different ways: (i) by first determining the  $t_{\text{Au}}$  by the  $\text{AuL}\alpha/\text{AuM}\alpha$  ratio and then getting  $t_{\text{In}}$  by the attenuated  $\text{InL}\alpha$  line transmitted by the gold layer or (ii) by using eqs. (1) to (7) with  $\text{InL}\alpha$  substituted by  $\text{NiK}\alpha$  and using  $\alpha_{\text{CuK}\alpha}^{\text{In}}$  and  $\alpha_{\text{InL}\alpha}^{\text{Au}}$  for the exponentials.

### V. EXPERIMENTAL RESULTS

To determine the thickness of the gold,  $t_{\text{Au}}$ , and nickel,  $t_{\text{Ni}}$ , layers (on the copper substrates), the number of counts (photons excited by fluorescence) in selected characteristic lines of the metallic layers and substrate are measured. The magnitude of the  $\text{CuK}\alpha$  and  $\text{NiK}\alpha$  lines from the sample are compared with the magnitude of the  $\text{CuK}\alpha$  and  $\text{NiK}\alpha$  lines produced by thick metallic plates of copper and nickel. The magnitude of the  $\text{AuL}\alpha$  line is also compared with the  $\text{AuL}\alpha$  line produced by a thick gold plate to obtain an approximate value of the gold thickness  $t_{\text{AUF}}$ . For gold films less than  $2 \mu\text{m}$  thick, the value of gold thickness  $t_{\text{Au}}$  obtained from the magnitude of the  $\text{CuK}\alpha$  and  $\text{NiK}\alpha$  lines when compared with  $t_{\text{AUF}}$  gives information on the physical characteristics of the gold film. If  $t_{\text{AUF}} \gg t_{\text{Au}}$ , the gold film may not be uniform in thickness due to pinholes or other defects.

The system calibration consists of two steps: (i) obtaining the values of the parameter  $\alpha$ 's defined in the last section and (ii) obtaining the magnitude of the characteristic lines corresponding to thick layers. For a given system geometry, the first step is done only once (when the system is set up). The second step is done as a routine check once a day (normally no changes are necessary over a period of several days). The second step could also be done only once if a reference signal ( $\text{PbL}\beta$ ) is utilized to compensate for variation in X-ray flux from the source.

Typical values of  $\alpha_{\text{NiK}\alpha}^{\text{Au}}$ ,  $\alpha_{\text{CuK}\alpha}^{\text{Au}}$ ,  $\alpha_{\text{CuK}\alpha}^{\text{Ni}}$  used in eqs. (5) and (6) as measured in our system are listed in Table I. The experiments were done by placing layers of gold and nickel (of known thicknesses) on



Table I

---

For $\theta_{\text{in}} = \theta_{\text{out}} = 45^\circ$
$\alpha_{\text{CuK}\alpha}^{\text{Au}} = 0.75$
$\alpha_1 = 0.84$
$\alpha_{\text{CuK}\alpha}^{\text{Ni}} = 0.15$
$\alpha_2 = 0.06$
$\alpha_3 = 4.87$
$\alpha_5 \approx 0.037$

---

copper or nickel substrates and comparing the magnitude of the  $\text{CuK}\alpha$  or  $\text{NiK}\alpha$  lines from the substrate with and without the layers. The value of  $\alpha_3$  was obtained from a known sample of nickel on a copper substrate for  $t_{\text{Au}} = 0$ . The values of  $\alpha_1$  and  $\alpha_2$  were obtained by measuring three standard samples in the range of 0.4 to 4  $\mu\text{m}$  provided by T. Briggs (Western Electric), which had been previously measured by atomic absorption. For  $\alpha = \alpha_{\text{NiK}\alpha}^{\text{Au}}$  (measured above) and  $\alpha_2 \approx 0.06$ , the three samples were measured with 5 percent of the nominal values for the gold films and within 10 percent of the nominal values for the nickel films. A more precise fit was not attempted due to the unknown tolerances of the standard samples.

The measurement time used for the standard samples was 100 s (real time). A 10- $\mu\text{s}$  pulse-shaping time constant was used in the amplifier and the pileup rejector. The count rate reaching the detector was about 1000 c/s with a 0.15-mA X-ray tube beam current at 50 kV. The target-to-sample distance was about 6 cm, and the detector-to-sample distance was about 1 cm.

To determine the reliability of the thickness measurements, the following experiment was performed. We measured several lead frame samples of the shape shown in Fig. 6. Each finger (16 per sample) was measured at the tip (dashed elliptical area in Fig. 4) and the thickness of gold and nickel were recorded. The measuring spot size was about  $125 \times 175 \mu\text{m}$ . Subsequently, the samples were measured by R. C. Kershner and N. Panousis at Bell Laboratories, Allentown by cross sectioning. The results are shown in Table II for the gold and Table III for the nickel.

The results performed using the X-ray technique were reproducible within  $\pm 2.4$  percent for the gold thicknesses and  $\pm 4$  percent for the nickel thicknesses in a series of 10 measurements (100 s each) in a given finger. The counting statistics were estimated to be  $\pm 1.2$  percent for the gold thickness measurements (7000 counts in the  $\text{CuK}\alpha$  line) and  $\pm 2.6$  percent for the nickel thickness measurements (1500 counts in the  $\text{NiK}\alpha$  line). Variations of  $\pm 10$  percent were observed along the tip of the fingers except for Sample 730 in which, due to off-centering of the plated pattern, larger variations were observed (as shown in Table II). The absolute accuracy of the X-ray measurements is mainly

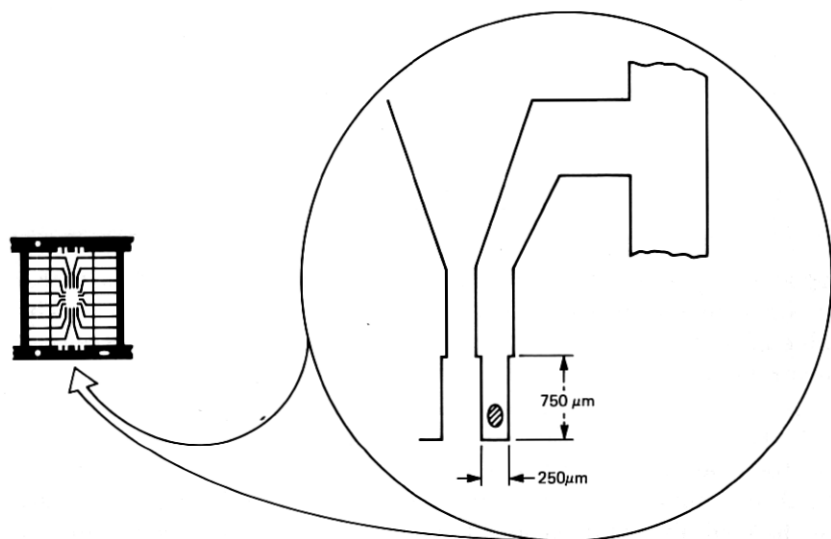


Fig. 6—Detail of lead frame. One of the fingers (leads) is magnified to show the effective area of X-ray measurement.

Table II—Au thickness ( $\mu$  inches)

Lead No.	Sample 730		Sample 801		Sample 822	
	X-Ray	Cross Section	X-Ray	Cross Section	X-Ray	Cross Section
1	112.6	110.2	99.3	93.9	155.8	151.1
2	97.4	109	99.4	103	143.3	149.3
3	104.5	113.8	104.6	112.6	140.3	151.7
4	63.8–115*	116.6	99.6	113.2	151.6	162.5
5	102.3	111.4	106.5	112.0	150.4	155.3
6	69.8–115.8*	112.6	108.9	98.7	158.5	157.7
7	103.6	94.5	96.8	99.9	153.1	139.7
8	92.8	109.6	96.2	101.7	159.3	152.3
9	100.8–116.8*	106.6	98.8	104.1	152.5	150.5
10	93.5	95.1	98.9	96.3	148.3	143.9
11	102.3	111.4	99.3	102.3	156.3	153.5
12	98	116.2	103.6	99.9	155	159.5
13	102.2	107.2	99.9	101.1	154.3	152.9
14	101.6	107.8	107.1	99.9	155	146.9
15	97.2	104.2	96.9	101.1	146.5	141.5
16	107.5	104.8	97	104.2	148.9	153.5

\* Uneven sample plating due to off-centering.

determined by the standard samples, the counting statistics, background corrections, and variations in system geometry. Due to the collimator design, the latter effect probably can be neglected. The scattering by the sample of the  $W\text{L}\alpha$  line from the source (very close in energy to the  $\text{CuK}\alpha$  line) precludes the use of background correction for the  $\text{CuK}\alpha$  line. However, background correction for the  $\text{NiK}\alpha$  line

Table III—Ni thickness ( $\mu$  inches)

Lead No.	Sample 730		Sample 801		Sample 822	
	X-Ray	Cross Section	X-Ray	Cross Section	X-Ray	Cross Section
1	24.7	18.7	19.4	11.4	30.3	19.3
2	22.8	15.7	20.1	12.0	28.9	21.7
3	25.8	15.7	21.3	14.5	29	20.5
4	22.2	15.7	20.7	13.8	31.3	22.9
5	23.9	15.1	21.5	15.7	29.9	22.3
6	25.9	15.1	22.9	10.8	30.2	25.5
7	23.7	15.7	19.8	13.8	29.6	18.1
8	22	16.3	19.3	13.2	31.1	19.9
9	27.6	15.7	20.4	12.6	29.2	19.9
10	23.7	16.3	20.3	13.2	29.5	23.5
11	24.7	16.3	19.2	13.8	30	19.3
12	23.2	14.4	20.8	12.6	31.2	19.9
13	23.2	14.5	19.7	14.5	31.5	22.3
14	23.4	13.2	20.7	13.8	31.3	22.3
15	23.6	17.5	19.3	11.4	29.6	23.5
16	25.5	16.3	18.1	12.0	28.7	16.9

is possible, but was not used in the reliability experiments. We assume that the standard samples are within  $\pm 5$  percent of the true value of gold thickness and within  $\pm 10$  percent of the true value of nickel thickness. The absolute accuracy of the X-ray measurements is about  $\pm 6$  percent for gold, in which background correction can be neglected, and  $\pm 11$  percent for nickel, also neglecting background correction. However, lack of  $\text{NiK}\alpha$  background correction could make the thin ( $<0.5 \mu\text{m}$ ) nickel films appear somewhat thicker. Automatic background correction for both gold and nickel thickness determinations is presently being done without increasing the measurement time, using a rhenium target X-ray tube (the  $\text{ReL}\alpha$  and the  $\text{CuK}\alpha$  lines are well separated).

When we compare the results shown in Tables II and III, we must bear in mind that the X-ray results indicate an average on a small, approximately elliptical, area while the cross-sectioning results indicate an average along a cord in the ellipse. Therefore, we do not expect complete agreement unless the films are uniform in the measured area. This was not always the case, since variations in thickness of  $\pm 10$  percent were observed along a given fingertip. These variations together with the accuracy of the measurements could show a spread in gold thicknesses of  $\pm 12$  percent and certainly an even larger spread for the nickel thicknesses. The cross-sectioning results shown in Table II are claimed to be within  $\pm 5$  percent of the true value. From Table II we observe that the maximum discrepancy between the two measuring techniques in any finger (not considering Sample 730, already discussed) was about 12 percent in Lead No. 4 of Sample 801. This result agrees very well with the estimated 6-percent accuracy of the X-ray

technique. The excellent agreement is substantiated by the fact that the correlation coefficient for both techniques (gold measurement) is 0.96, taking the higher values with asterisk in Sample 730. The correlation coefficient was calculated comparing the three samples (48 measurements in each technique). The accuracy of the nickel thicknesses obtained by cross-sectioning was claimed to be  $\pm 50$  percent. Therefore, very good agreement is not expected in Table III. However, we observe from the table that both techniques indicate that Sample 801 has the thinnest nickel film and Sample 822 has the thickest. The correlation coefficient for the nickel film measurements is about 0.9.

## VI. CONCLUSIONS

In this paper, we demonstrated the capabilities of monitoring the thickness of small areas of gold and nickel thin films deposited on copper substrates, in time less than 20 s. The accuracy of the system depends on the measuring time and also on the accuracy of the standard samples used to calibrate the system. One possible source of error is the variation in distances among the sample, the detector, and the X-ray source. This has been minimized by the design of a special lead collimator to fix the geometry of the system. The collimator also maximizes the detector solid angle relative to the sample to decrease the measuring time. (This variation could also be eliminated as described above by utilizing the ratios of the fluorescent lines.)

Shorter measurement times can be obtained either by using a pulsed X-ray source to decrease system dead time or by using a faster X-ray analyzer. Increasing the spot size probably would also be worthwhile in order to obtain a more meaningful average on a given sample due to nonuniformity of metallization. Finally, the system described in this paper also has the capability of chemical qualitative analysis.

## VII. ACKNOWLEDGMENTS

The authors wish to thank G. A. Coquin and D. R. Herriott for many helpful discussions, C. J. Schmidt for constructing the detector collimator and technical assistance, W. Flood and C. Steidel for providing the lead frame samples. T. Briggs\* of Western Electric (Allentown) for providing the standard samples, and R. Kershner and N. Panousis for the cross-section measurements.

---

\* T. Briggs has built a thickness measuring production system based on the prototype described in this paper. The system is presently being used at the Western Electric facility in Allentown, Pa., for monitoring lead frames used in packaging integrated circuits.

## APPENDIX A

### *CuK $\alpha_{12}$ Fluorescence Counting Rate in the Reflection System*

The CuK $\alpha_{12}$  fluorescence in the reflection system can be obtained using Fig. 4. The incident X-rays from the source subtending a solid angle  $\sigma_{in}$  are partially absorbed by the gold and nickel films and then by the copper substrate. At any depth  $x$ , these X-rays excite isotropic fluorescent K $\alpha_{12}$  radiation from an element of volume of thickness  $dx$  equal to

$$dN_{CuK\alpha} = 1.66 \times 10^{12} \sigma_{in} \sigma_{out} I \int_{8.3}^{V_0} \sin \theta_{in} \frac{\mu_{Cu} \rho_{Cu}}{\exp(-\mu_w \rho_w t_w)} \\ \times \left( \frac{V_0}{V} - 1 \right) \exp[-(\mu_{Cu} \rho_{Cu} \text{CSC } \theta_{in} + \mu_{Cu}^{CuK\alpha} \rho_{Cu} \text{CSC } \theta_{out})] \\ \times \exp[-(\mu_{Ni} \rho_{Ni} \text{CSC } \theta_{in} + \mu_{Ni}^{CuK\alpha} \rho_{Ni} \text{CSC } \theta_{out}) t_{Ni}] \\ \times \exp[-(\mu_{Au} \rho_{Au} \text{CSC } \theta_{in} + \mu_{Au}^{CuK\alpha} \rho_{Ni} \text{CSC } \theta_{out}) t_{Au}] dV, \quad (9)$$

where  $\sigma_{out}$  is the detector solid angle,  $\sigma_{in}$  and  $\sigma_{out}$  are defined in Fig. 4, and the mass absorption coefficients of the different materials to the CuK $\alpha_{12}$  radiation have been considered. The expression given by Kramers<sup>3</sup> for the continuum radiation from a tungsten target has been used in the calculations.

For source-to-sample and sample-to-detector distances, large relative to the copper substrate effective thickness ( $\sim 30 \mu\text{m}$ ), we can write for the total CuK $\alpha_{12}$  radiation reaching the detector:

$$N_{CuK\alpha_{12}} = 1.66 \times 10^{12} \sigma_{in} \sigma_{out} I \\ \times \int_{8.3}^{V_0} \frac{\mu_{Cu} \rho_{Cu} (V_0/V) \exp(-\mu_w \rho_w t_w)}{\sin \theta_{in} (\mu_{Cu} \rho_{Cu} \text{CSC } \theta_{in} + \mu_{Cu}^{CuK\alpha} \rho_{Cu} \text{CSC } \theta_{out})} \\ \times (1 - \exp[-(\mu_{Cu} \rho_{Cu} \text{CSC } \theta_{in} + \mu_{Cu}^{CuK\alpha} \rho_{Cu} \text{CSC } \theta_{out}) t_{Cu}]) \\ \times \exp[(\mu_{Ni} \rho_{Ni} \text{CSC } \theta_{in} + \mu_{Ni}^{CuK\alpha} \rho_{Ni} \text{CSC } \theta_{out}) t_{Ni}] \\ \times \exp[-(\mu_{Au} \rho_{Au} \text{CSC } \theta_{in} + \mu_{Au}^{CuK\alpha} \rho_{Ni} \text{CSC } \theta_{out}) t_{Au}] dV, \quad (10)$$

where the  $\times$  integration through the copper substrate was already performed. The results obtained from eq. (9) are presented in Fig. 5 for two different cases.

## APPENDIX B

### *Calculation of the Direct AuL $\alpha$ Fluorescence*

The model used for the following calculations is based on Fig. 4 with the copper substrate substituted by the gold film and by eliminating

any additional films. Integrating through the gold thickness, the AuL $\alpha$  fluorescence counting rate is given by

$$N_{\text{AuL}\alpha} = 4.7 \times 10^{11} B \int_{11.9}^{V_0} \frac{(V_0/V - 1)}{B/V^{2.7} + 0.275(\sin \theta_{\text{in}}/\sin \theta_{\text{out}})} \\ \times \left( 1 - \exp \left[ - \left( \frac{B \csc \theta_{\text{in}}}{V^{2.7}} + 0.275 \csc \theta_{\text{out}} \right) t_{\text{Au}} \right] \right) \\ \times \frac{1}{V^{2.7}} \exp(-380 t_w / V^{2.65}) dV,$$

where a  $W$  target of thickness  $t_w(\mu\text{m})$  is assumed and where  $B$  is a parameter which defines  $\mu_{\text{Au}}$  between the different  $L$  absorption edges.  $B = 297.9$  for  $11.9 \leq V < 13.7$ ,  $B = 410$  for  $13.7 \leq V < 14.3$ , and  $B = 570.4$  for  $14.3 \leq V \leq V_0$ . The results are shown in Fig. 5 of the text.

## REFERENCES

1. H. A. Liebhafsky, et al., *X-Ray Absorption and Emission in Analytical Chemistry*, New York: John Wiley & Sons, 1960.
2. R. H. Zimmerman, "Industrial Applications of X-Ray Methods for Measuring Plating Thickness," *Advances in X-Ray Analysis*, 4, 1961, p. 335.
3. H. A. Kramers, *Phi. Mag.*, 46, 1923, p. 836.